

# Modeling Covalent-Modifier Drugs

Ernest Awoonor-Williams, Andrew G. Walsh, and Christopher N. Rowley  
*Memorial University of Newfoundland, St. John's, Newfoundland and Labrador, Canada*

---

## Abstract

In this review, we present a summary of how computer modeling has been used in the development of covalent modifier drugs. Covalent modifier drugs bind by forming a chemical bond with their target. This covalent binding can improve the selectivity of the drug for a target with complementary reactivity and result in increased binding affinities due to the strength of the covalent bond formed. In some cases, this results in irreversible inhibition of the target, but some targeted covalent inhibitor (TCI) drugs bind covalently but reversibly. Computer modeling is widely used in drug discovery, but different computational methods must be used to model covalent modifiers because of the chemical bonds formed. Structural and bioinformatic analysis has identified sites of modification that could yield selectivity for a chosen target. Docking methods, which are used to rank binding poses of large sets of inhibitors, have been augmented to support the formation of protein-ligand bonds and are now capable of predicting the binding pose of covalent modifiers accurately. The  $pK_a$ 's of amino acids can be calculated in order to assess their reactivity towards electrophiles. QM/MM methods have been used to model the reaction mechanisms of covalent modification. The continued development of these tools will allow computation to aid in the development of new covalent modifier drugs.

*Keywords:* review, covalent modifiers, irreversible inhibition, computer modeling, docking, QM/MM, bioinformatics,  $pK_a$ , cysteine, Michael addition, kinase

---

## 1. Introduction

The general mechanism for the inhibition of an enzyme or receptor by a small molecule drug is for the drug to bind to the protein, attenuating

*Preprint submitted to Biochimica et Biophysica Acta: Proteins and Proteomics May 10, 2017*

4 its activity. The canonical mode by which a drug will bind to its target is  
5 through non-covalent interactions, such as hydrogen bonding, dipole–dipole  
6 interactions, and London dispersion interactions. Kollman and coworkers  
7 estimated that small molecules that bind to proteins through non-covalent  
8 interactions have a maximum binding affinity of 6.3 kJ/mol per non-hydrogen  
9 atom [1], so these binding energies are generally sufficiently weak for the  
10 binding to be reversible. This establishes a measurable equilibrium between  
11 the bound and unbound states.

12 A sizable class of drugs bind to their targets by an additional mode; a co-  
13 valent bond is formed between the ligand and its target. These drugs contain  
14 a moiety that can undergo a chemical reaction with an amino acid side chain  
15 of the target protein, covalently modifying the protein. Dissociating this co-  
16 valent modifier from the target requires these protein–ligand bonds to be bro-  
17 ken. In the cases where the dissociation is strongly exergonic, the equilibrium  
18 will lie so far towards the bound state that the inhibition is effectively irre-  
19 versible. Some covalent protein–ligand reactions are only weakly exergonic,  
20 so covalent modification can be reversible in some instances [2]. These ligands  
21 also interact with the protein through conventional non-covalent intermolec-  
22 ular forces, so the total binding energy in the covalently-bound state results  
23 from both covalent and non-covalent interactions. Refs. [3, 4, 5, 6, 7, 8] are  
24 recent reviews on covalent-modifier drugs.

25 The covalent modification of proteins can involve many types of chemical  
26 motifs in the inhibitor and involve a variety of amino acids. Catalytic residues  
27 in the active site often have depressed  $pK_a$ 's, so they are more likely to  
28 occupy the deprotonated state that is reactive towards electrophiles. Serine  
29 residues that serve as a Brønsted acid in an enzymatic catalytic cycle have  
30 been a popular target. Two of the most famous covalent modifier drugs  
31 (Figure 1) act by acylating this type of active-site serine residue; aspirin  
32 targets Ser530 of cyclooxygenase and penicillin targets DD-transpeptidase.  
33 Catalytic serines, threonine, and cysteine residues have all been targeted by  
34 covalent modifiers [9].

35 In recent years, there have been extensive efforts to develop covalent  
36 modifier drugs that undergo reactions with the thiol group of non-catalytic  
37 cysteine residues. Cysteines are relatively rare amino acids, comprising only  
38 2.3% of the residues in the human proteome [10]. This limits the number of  
39 off-target reactions that are possible. These non-catalytic residues are less  
40 likely to be conserved within a family of proteins, which creates opportunities  
41 to select for a specific target in a large family of proteins. Although this type

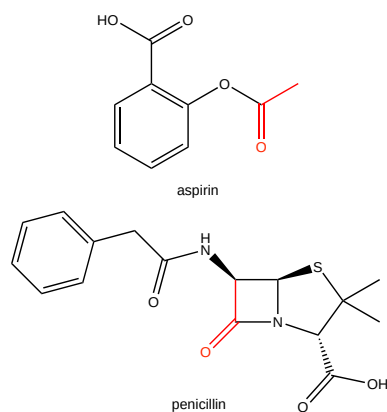


Figure 1: Aspirin and penicillin are early examples of covalent modifier drugs. These drugs bind to their target by acetylating a catalytic serine residue. The reactive moiety is drawn in red.

of covalent modification does not inactivate the catalytic residues directly, the covalent linker serves to anchor the drug binding site and achieve a stronger binding affinity. Large-scale screens have shown that reactive fragments have unexpectedly high specificity for individual proteins, suggesting that covalent modifiers have a lower risk of promiscuity than had been assumed [11, 12, 13].

These advantages must be balanced against the drawbacks associated with covalent protein–ligand binding. Covalent protein–ligand adducts are believed to trigger immune responses in some cases [14]. Further, the inhibitor must be carefully tuned so that it will only bind irreversibly to its target because irreversible inhibition of an off-target receptor could result in adverse drug reactions. The chemical reactivity of the warhead also creates the potential that the inhibitor will be chemically degraded in an inactive form through metabolism or other types of chemical reactions before it reaches the target. This constrains the reactivity of the warhead.

To develop drugs of practical use that have the advantages of covalent modification but avoid the disadvantages, researchers have developed targeted covalent inhibitors (TCIs). Typically, these compounds have a non-covalently binding framework that is highly selective for the target. For example, covalent modifier ibrutinib (Figure 2) shares the diaminopyrimidine scaffold that has been successfully employed in the development of Bruton’s tyrosine kinase-selective non-covalent inhibitors. The reactive warhead is an acrylamide, which is a moderately-reactive electrophile. Thio-Michael

additions are generally only weakly exergonic, so these additions are often reversible [15]. This allows the inhibitor to dissociate if it reacts with a thiol of a protein other than its target. High selectivity is achieved by the combination of selective non-covalent interactions and the additional strength of the covalent interaction between the warhead and a complementary reactive amino acid.

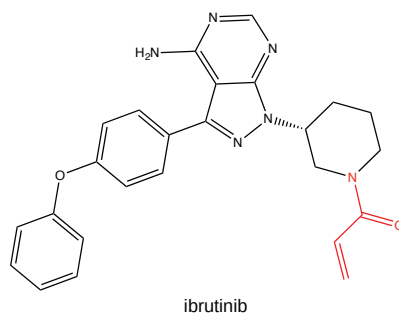
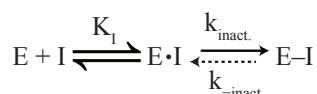


Figure 2: Ibrutinib is an example of a targeted covalent inhibitor. The reactive acrylamide warhead is indicated in red.

### 1.1. Physical Parameters of Covalent Modification

The strength of the binding of a non-covalent inhibitor to its target can be quantified by the equilibrium constant,  $K_I$ , for the association of the ligand (inhibitor, I) and its target (enzyme, E) to form a protein–ligand complex (E·I). This association can also be defined in terms of the Gibbs energy of binding through the relation  $\Delta G_{non-covalent} = -RT \ln K_I C^\circ$ , where  $C^\circ$  is the standard state concentration [16]. The binding of a covalent modifier involves additional steps. The protein–ligand complex (E·I) undergoes reaction to form the covalent adduct (I–E). The rate of this process is characterized by its rate constant,  $k_{inact.}$ . In some cases, this reaction is reversible and the covalent adduct can revert to the non-covalent protein–ligand complex with the rate constant  $k_{-inact.}$ . If the reaction is strongly exergonic,  $k_{inact.}$  will be much larger than  $k_{-inact.}$ , so the binding will effectively be irreversible. The total binding energy of the ligand results from both the covalent and non-covalent protein–ligand interactions ( $\Delta G_{non-covalent}$ ).

The rate at which an inhibitor reacts with the target ( $k_{inact.}$ ) can be calculated using transition state theory. Conventional transition state theory is the simplest and most widely used theory, which relates the rate of reaction



to the Gibbs energy profile along the reaction coordinate<sup>1</sup>. Using transition state theory, the rate of reaction can be calculated by the Gibbs energy of activation ( $\Delta G^\ddagger$  of the rate limiting step [18]),

$$k_{TST} = \frac{k_B T}{h} \exp \left( \frac{-\Delta G^\ddagger}{k_B T} \right). \quad (1)$$

The mechanism of covalent modification can be complex and involve multiple reaction steps. For example, the mechanism of covalent modification of a cysteine by a Michael acceptor involves the deprotonation of the thiol to form a thiolate, formation of an enolate intermediate, and protonation of the enolate to form the thioether product (Figure 4). A comprehensive model for covalent modification would require calculation of  $\Delta G_{non-covalent}$ ,  $\Delta G_{covalent}$ , as well as the rate-limiting barriers of the chemical reaction ( $\Delta G^\ddagger$ ). The rates binding, unbinding, inactivation, and activation govern the drug residence time, which has been proposed to be a better determinant of in vivo pharmacological activity than the binding affinity [19, 20, 21].

### 1.2. Computer Modeling in Drug Discovery

Computer modeling is used extensively in the pharmaceutical industry to aid in the development of new drugs. The membrane permeability of a drug can be estimated by empirical computational methods or molecular simulation [22, 23, 24]. Docking algorithms are used to rapidly screen large databases of compounds for their ability to bind a protein or nucleic acid that is targeted for inhibition [25, 26, 27]. Other methods, such as free energy perturbation (FEP), are used to calculate the binding affinities of a drug to a protein ( $\Delta G_{non-covalent}$ ) [28, 29, 30, 31]. These methods are generally based on molecular mechanical force fields or other simplified representations of the protein and ligand, which typically only describe the intermolecular component of protein–ligand binding. Covalent modification inherently involves the making and breaking of chemical bonds, so these methods must be

<sup>1</sup>A discussion of the limitations of this model in enzymatic reactions is available in Ref. 17.

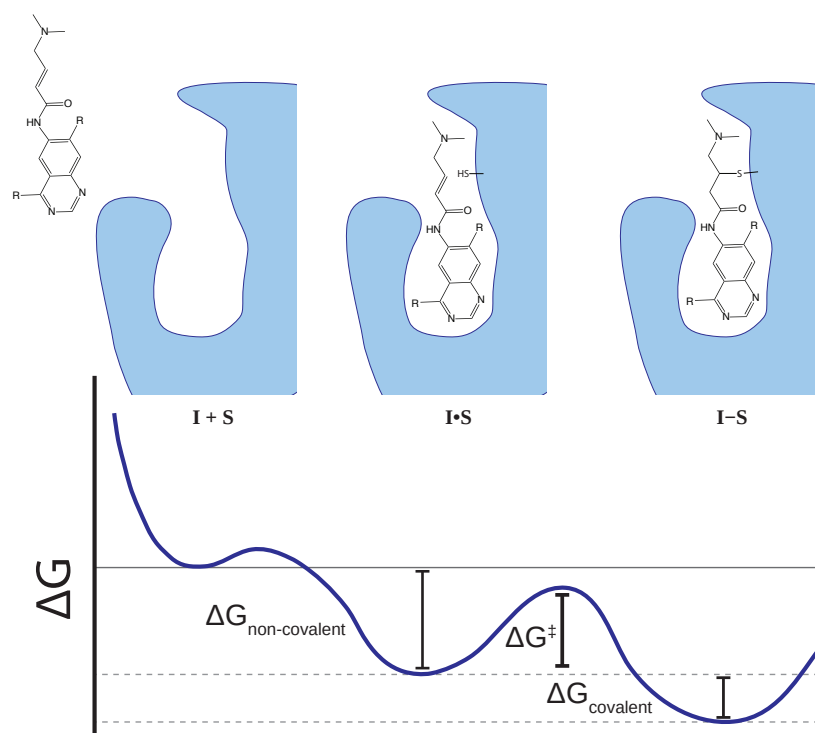


Figure 3: Schematic binding profile for the formation of a covalent protein–ligand complex. In this example, afatinib binds non-covalently to the active site of EGFR (I•S), then undergoes a chemical reaction with the thiol group of Cys-797 to form a covalent thioether adduct (I–S).

114 adapted to describe this mode of binding. In this review, we present methods  
 115 for modeling covalent-modifier drugs. Another recent review is available in  
 116 Ref. [32].

## 117 2. Structural Analysis

118 The Protein Data Bank (PDB) now contains over 100,000 biological  
 119 macromolecular structures [33]. These data have been invaluable for the  
 120 development of covalent-modifier drugs. Cocrystals showing covalent bond  
 121 formation between covalent-modifier drugs have helped confirm these drugs  
 122 act as covalent modifiers and unambiguously indicate the site of modification.  
 123 For example, Figure 5 shows the covalent binding of ibrutinib to *Toxoplasma*  
 124 *gondii* calcium-dependent protein kinase 1 (TgCDPK1). The availability

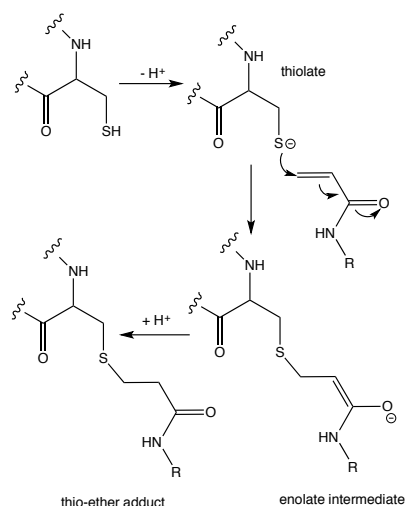


Figure 4: The mechanism of the addition of an acrylamide warhead to a cysteine thiol.

125 of these structures has enabled structure-based design of covalent modifiers  
 126 through docking and mechanistic modeling.

127 This structural data is particularly valuable for designing drugs that are  
 128 selective for one member of a family of structurally similar targets. The  
 129 protein kinase family is a prototypical example of this. This family contains  
 130 hundreds of members with a large degree of structural similarity in their  
 131 kinase domains. Due to their roles in cell signaling and division, individ-  
 132 ual members of this family are drug targets, but there is a significant risk  
 133 of adverse drug reactions due to inhibition of other kinase proteins with a  
 134 structurally-similar active-site [34]. Several kinase-targeting covalent modi-  
 135 fers have been developed, which have the potential for higher affinity and  
 136 selectivity [35, 36]. Structural analysis of the available kinase structures has  
 137 been essential for identifying poorly-conserved druggable residues within the  
 138 active site of the target, which allows a covalent-modifier to be designed with  
 139 a warhead in a complementary position.

140 Cohen et al. reported an early structural study where a covalent-modifier  
 141 drug was designed to selectively inhibit the RSK1 and RSK2 protein kinases  
 142 [37]. Proteins in the kinase family have been selectively targeted by non-  
 143 covalent inhibitors because a residue, known as the gatekeeper, can block  
 144 binding of the ligand to a hydrophobic pocket in the active site. Inhibitors  
 145 with a hydrophobic group that binds to this pocket will be selective for

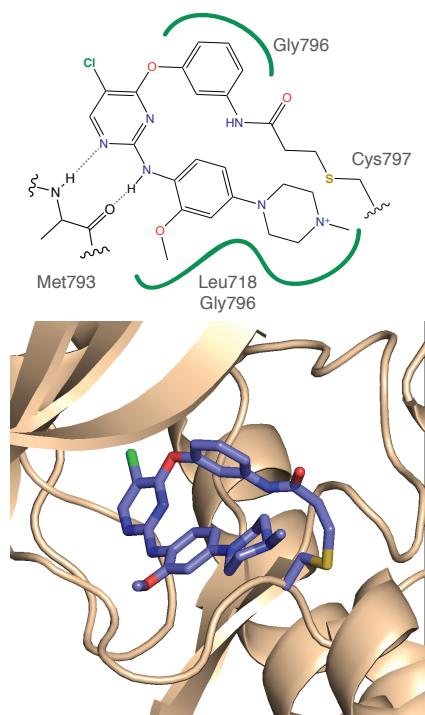


Figure 5: Ibrutinib bound to TgCDPK1 (PDB ID: 4IFG). The acrylamide warhead has undergone a Michael addition with the thiol group of Cys-797, forming a covalent thioether adduct between the protein and the ligand. Non-covalent interactions also stabilize the protein–ligand complex.

146 these kinases. The RSK1, RSK2, and Src kinase all have a small threonine  
 147 gatekeeper, so they all bind inhibitors of this class with similar affinity. A  
 148 non-conserved cysteine is present in the glycine-rich loop on the N-terminal  
 149 lobe adjacent to the binding site in RSK1 and RSK2, which is absent in  
 150 Src. A pyrrolopyrimidine ligand with a fluoromethylketone warhead was  
 151 synthesized, where the non-covalent interactions are optimal for a threonine-  
 152 gatekeeper binding site and the warhead is situated such that it will react  
 153 with the loop cysteine residue of RSK1 and RSK2. This molecule was found  
 154 to selectively inhibit RSK1 and RSK2 by covalent modification, but had a  
 155 lower affinity for other Src kinase proteins that lacked a cysteine residue at  
 156 the targeted position. This is illustrated by docked structures in Figure 6.

157 Zhang et al. performed a more extensive bioinformatic analysis of the hu-  
 158 man kinase family and found that approximately 200 members of the family



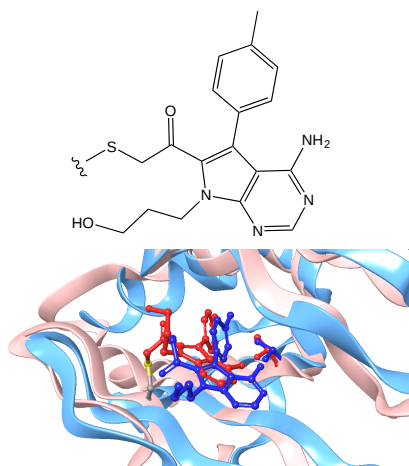


Figure 6: Docked structures of the pyrrolopyrimidine fluoromethylketone ligand (fmk) of Cohen et al. [37] bound to RSK2 (red, PDB ID: 2QR8) and c-Src kinase (blue, PDB ID: 3F6X). Both proteins have a threonine in the gatekeeper position, limiting the selectivity that can be achieved by existing non-covalent inhibitors. Fmk binds selectively to RSK2 by forming a covalent bond to with a non-conserved cysteine residue (Cys-436). A valine residue (Val-281) holds this position in c-Src.

159 had a cysteine residue in the vicinity of the binding site [38]. These proteins  
 160 were divided into 4 groups based on the general areas of the binding site  
 161 where the cysteine is located. These residues are not highly conserved across  
 162 the family, so covalent modification that targets one of these residues will be  
 163 selective for a small subset of the kinase family.

164 A structural analysis by Leproult et al. of the active sites of kinase pro-  
 165 teins also showed that there was significant variation in the location of active  
 166 site cysteine residues [39]. The available crystal structures of human kinases  
 167 were grouped into three conformational classifications: active, inactive C-  
 168 helix-out, and inactive DFG-out. This analysis showed that there is a large  
 169 number of targetable cysteines in the kinase family, so the strategy of de-  
 170 signing a targeted covalent inhibitor could have wide application for these  
 171 drug targets. Non-covalent inhibitor imatinib binds to the DFG-out confor-  
 172 mation of ABL1, KIT, and PDGFR $\alpha$  kinases, but has the highest affinity  
 173 for KIT kinase. The authors synthesized variants of imatinib with different  
 174 electrophilic warheads. These inhibitors had a lower affinity for ABL1, but  
 175 had a higher affinity for KIT and PDGFR $\alpha$ . The new inhibitors were shown  
 176 to bind non-covalently to these proteins.

177 These structural studies of the kinase family highlight the potential of  
178 TCIs. The catalytic-domain binding sites of the human protein kinase fam-  
179 ily has limited structural variation, so it is difficult to design a selective  
180 inhibitor. Targeted covalent modifiers can be designed by adding an elec-  
181 trophilic warhead to existing non-covalent drug scaffolds. This warhead can  
182 only form a covalent linkage with a cysteine residue at a complementary po-  
183 sition. Only a small number of proteins in the kinase family have a cysteine  
184 residue at this position, so binding to this site by a covalent addition is selec-  
185 tive for a small number of kinases. This design principle may also be effective  
186 to achieve selectivity for a target in a family of similar proteins.

187 Wu et al. generalized this type of analysis by constructing a web-based  
188 database of known covalently-bound structures collected from structural and  
189 literature databases[40]. At the time of its public release, the database con-  
190 tained 462 protein structures and 1217 inhibitors. This searchable database  
191 hyperlinks to entries in the PDB for the protein–ligand complex and to chem-  
192 ical database entries (e.g., UniPROT) of the ligands. For each druggable  
193 cysteine, the solvent-accessible surface area (SASA) and conservation within  
194 its family are also reported. The calculated  $pK_a$  of the residue is also re-  
195 ported, although these calculations were performed using the PROPKA3.1  
196 package, which has poor accuracy for cysteine residues [41]. The database is  
197 accessible through the URL: <http://www.cysteinome.org/>.

198 Most recently, Bourne and coworkers applied the functional-site inter-  
199 action fingerprint (Fs-IFP) method to classify the binding modes of known  
200 kinase inhibitors. The Fs-IFP method analyzes the crystallographic structure  
201 of a protein–ligand complex into a bit-string, allowing diverse protein–ligand  
202 complexes to be classified systematically [42]. The researchers analyzed 2774  
203 structures of protein–ligand complexes of kinases [43]. 1599 structures were  
204 found to have one or more cysteine residues in the binding site, which cor-  
205 responded to 169 different kinases that could, in principle, be targeted by  
206 a covalent modifier. 17 cysteine residues were found to be in close contact  
207 with an inhibitor in the published structures. Based on this analysis, cys-  
208 teine residues on the P-loop, catalytic group, DFG loop, roof, and front of  
209 the kinase binding sites were identified as being accessible for covalent modi-  
210 fication. Conversely, cysteine residues on the hinge region were concluded to  
211 have a poor orientation or to be too inaccessible to be suitable targets.

### 212 3. Docking Algorithms

213 There are many established codes that can screen databases of small  
214 molecules for the ability to bind to a protein. For large numbers of com-  
215 pounds to be screened in a tractable period of time, these methods use highly  
216 efficient algorithms to estimate if a molecule has the appropriate geometry to  
217 bind to the target site. These docking algorithms also assign “scores” to the  
218 various binding poses based on estimates of the intermolecular interactions  
219 in the bound state. To allow high throughput screens of a large databases of  
220 compounds, these models are generally highly simplified, so the calculated  
221 interaction scores serve to rank the poses approximately and are not rigorous  
222 Gibbs energies of binding.

223 Conventional docking methods were developed to describe non-covalent  
224 protein–ligand interactions, so the stabilization that occurs through the covalent  
225 bond formation is not included by these algorithms. Moreover, covalent  
226 linkage places the ligand at a short distance from the covalently-modified  
227 residue, which is strongly disfavored by the standard steric repulsion terms  
228 in non-covalent docking algorithms. The covalent linkage also imposes addi-  
229 tional constraints on the pose due to the geometry of warhead-residue bond.  
230 To address these issues, new methods have been developed to model the  
231 covalent docking of a ligand with the protein (Table 1).

Table 1: Algorithms for predicting covalent-binding poses and the programs they are implemented in.

Algorithm	Program	Reference
MacDOCK	DOCK/MIMIC	44
FITTED	FORECASTER	45
DOCKovalent	DOCK Blaster (web)	46
CovDock	Glide/Prime	47
CovDock-VS	Glide	48
Two-point attractor / flexible side chain	AutoDock	49
DOCKTITE	MOE	50

232 Support for covalent docking has been implemented into the FITTED  
233 modeling suite [51, 52, 45]. Compounds containing appropriate reactive war-  
234 heads are identified from the ligand database. Poses where the warhead is  
235 in close proximity to a reactive amino acid are automatically identified and  
236 used to construct a covalently-bound adduct. This approach uniquely allows

both covalent and non-covalent binding models to be identified simultaneously and automatically. The binding poses are ranked by the RankScore and MatchScore algorithms. This methodology was used to identify novel covalent inhibitors of prolyl oligopeptidase that exhibited high selectivity and affinity to Ser554 [53, 54, 55].

Del Rio et al. developed a computational workflow for evaluating the binding of a covalent modifier to a protein [56]. A database of kinase proteins with non-covalently-bound structures was constructed from the Protein Data Bank. From these structures, inhibitors bound near cysteine residues that had strong non-covalent binding energies were selected. These structures were used as scaffolds for the design of new inhibitors with electrophilic warheads that bind near cysteine residues. The covalently-bound protein–ligand complexes for these compounds were constructed and simulated using molecular dynamics. Inhibitors which required a large distortion in the protein structure in order to form the covalent ligand were rejected.

Ouyang et al. developed CovalentDock by modifying AutoDock5.2 [57]. This method is distinct from some other codes because ligand–protein interaction potential explicitly includes the energy of the covalent linkage. This linkage is described using a Morse potential, where the potential energy minimum forms a covalent bond but the bond can form or dissociate dynamically. This program is also available through a web-based interface, CovalentDock Cloud [58].

London et al. developed the DOCKoValent docking algorithm for covalent docking using the web-based docking server DOCK Blaster [46]. This server uses a library of electrophile-containing ligands, including  $\alpha$ ,  $\beta$ -unsaturated carbonyls, aldehydes, boronic acids, cyanoacrylamides, alkyl halides, carbamates,  $\alpha$ -ketoamides, and epoxides. These ligands were modified to assume the geometry they will hold when covalently bound to the target. A set of likely rotamers is generated for each compound. To search for stable binding poses, protein–ligand complexes are generated where the protein–ligand linkage is constrained to its ideal geometry. The DOCK3.6 scoring algorithm is used to rank the ligands. This method was successfully applied to a novel inhibitor of AmpC  $\beta$ -lactamase, where a covalent bond is formed between a boronic acid warhead and the catalytic serine residue. It was also effective at finding drugs capable of binding to kinase proteins RSK2, MSK1, and JAK3 through reaction of ligands containing a cyanoacrylamide warhead with non-catalytic cysteine residues in or near the active site (Cys436 in RSK2, Cys440 in MSK1, and Cys909 in JAK3).

275 Bianoco et al. recently implemented two covalent docking algorithms  
 276 into AutoDock4, a widely-used docking program [59]. The first algorithm is  
 277 the two-point attractor method, where an artificial potential is defined that  
 278 favors overlap between two artificial sites attached to the warhead of covalent  
 279 modifiers to the  $C_{\beta}$ -O sites of a target serine or the  $C_{\beta}$ -S sites of a target  
 280 cysteine. This allows the drug to move freely in the active site, while favoring  
 281 conformations where the ligand is in a covalently-bound pose. The second  
 282 algorithm treats the ligand as a flexible side chain of the protein. The flexible  
 283 side chain method predicted the RMSD of bound poses in better agreement  
 284 with the experimental structures than the two site model.

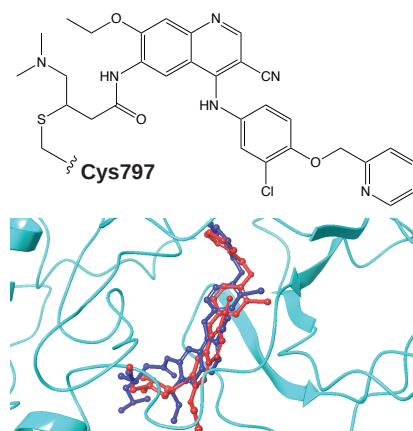


Figure 7: Binding of neratinib (HKI-272) to EGFR modeled using CovalentDock. The RMSD of the non-hydrogen atoms of the ligand are 2.14 Å with respect to the experimental crystallographic structure (PDB ID: 2JIV). The experimental and predicted ligand poses are colored in red and blue, respectively.

285 The Glide docking program developed by Schrödinger Inc. has also been  
 286 modified to support modeling covalent binding ligands [47]. This algorithm  
 287 mutates the target residue into an alanine residue and performs a conven-  
 288 tional docking simulation to generate a library of hundreds of poses. These  
 289 poses are filtered to select those where the warhead is within 5 Å of the  
 290 target residue based on a rotamer library. Covalently-bound structures are  
 291 generated from these bound poses. Further optimization and clustering is  
 292 performed on these poses using the Prime refinement program [60, 61], which  
 293 are ranked to yield a final optimal binding pose. Ligands can be screened  
 294 by calculating an apparent affinity, which is estimated from the average of  
 295 the scores for the covalently-bound and non-covalently-bound poses. On a

test set of 38 covalently-bound protein–ligand complexes, this method was able to predict the binding pose with an RMSD of 1.52 Å from the experimental crystallographic structure. An example of the predicted pose of a covalently-bound inhibitor using this method is presented in Figure 7.

Warshaviak modified the CovDock workflow to enable fast structure-based virtual screening of covalent modifiers [48]. In the CovDock-VS workflow, the target residue is also mutated into an alanine, but a restraint is imposed so that the warhead remains within 5 Å of the target residue during the conformational search. This restricts the initial search so that only poses where covalent bond formation is possible are identified. Covalently-bound structures are generated from these poses, energy-minimized, then clustered to identify unique poses. These poses are directly scored using the GlideScore algorithm, omitting the additional structural refinement stage in CovDock. This simplified workflow had a throughput that was 10–40 times faster than CovDock but the mean RMSD of predicted binding poses for the test set of 21 structures only increased to 1.87 Å from the 1.52 Å RMSD of the original CovDock workflow.

Ai et al. presented a technique steric-clashes alleviating receptor (SCAR) [62], where the covalently-binding residue is mutated into a sterically smaller residue, such as serine or glycine. This allows the ligand to dock in poses similar to the covalently-modified mode without experiencing a steric clash. These poses are ranked according to their non-covalent binding score. This procedure was evaluated by comparing the predicted pose to the experimental crystallographic structures of covalently-inhibited AdoMetDC. This technique predicted the binding pose with an RMSD of 3.0 Å, which is comparable to other covalent docking methods. In their complete workflow, the ensemble of docked poses was filtered to select those where the warhead was within 1 Å of the targeted residue. The mean RMSD of the top-ranked structures after imposing this constraint was reduced to 1.9 Å. This procedure was successfully applied to discover novel covalent inhibitors of S-adenosylmethionine decarboxylase.

Scholz et al. presented the implementation of DOCKTITE [50], a covalent docking method into the Molecular Operating Environment (MOE [63]) modeling suite. This method searches a database of potential ligands for molecules possessing one of 21 electrophilic warhead motifs. The structure of the ligand is adjusted to reflect its structure when covalently-bound. Constraints are imposed to force the ligand to occupy a geometry consistent with a covalent linkage and a conformational search is performed to identify the

low-energy poses of the ligand in the receptor. Of the 76 covalent-modifier test set developed by Oyang et al., the top-ranked pose predicted by DOCK-TITE was 2.4 Å, comparable to other covalent-docking methods. A recent application of DOCKTITE was reported by Schirmeister et al., who found that the relative affinities of covalently-binding dipeptide nitriles inhibitors of rhodesain were correctly predicted by the calculated affinity scores [64].

These implementations have made the docking of covalent-modifiers drugs practical and accessible, although further development of these methods is still needed. Databases containing drugs with warheads must be developed and the codes must be able to identify the potential modes of modification. In some of these codes, the user is required to provide the site of covalent modification, so the screening performed by this code is not yet fully automatic. The energy associated with covalent bond formation (i.e.,  $\Delta G_{covalent}$ ) is not immediately available in conventional scoring algorithms, so the absolute strength of binding cannot be realistically estimated by these algorithms either.

#### 4. Calculation of the pKa's of Targeted Residues

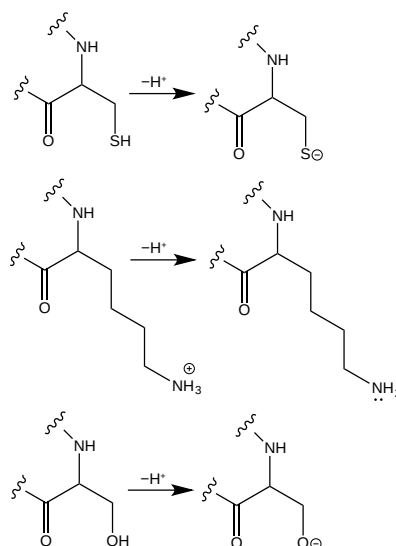


Figure 8: Deprotonation reactions involving cysteine, lysine, and serine. Covalent modification of these residues typically involves reaction in their deprotonated, nucleophilic states.



351 Generally, the first step in the mechanism for covalent modification of  
352 cysteines, lysines, and serines is their deprotonation to yield their more reac-  
353 tive form (Figure 8). In the case of the modification of a cysteine residue by  
354 an electrophile, the thiol group of the amino acid side-chain must be deproto-  
355 nated to form the reactive thiolate nucleophile. The stability of the thiolate  
356 is thus a significant parameter for the inhibition of a target site by a drug  
357 molecule.

358 The equilibrium between the thiol and thiolate states of a cysteine residue  
359 in a protein is defined by its  $pK_a$ . Cysteines with low  $pK_a$ 's are more likely  
360 to exist in their reactive thiolate state, so they will be more susceptible  
361 to covalent modification by electrophilic inhibitors. The standard  $pK_a$  of a  
362 cysteine residue is 8.6 [65], but  $pK_a$ 's of cysteines have been reported to range  
363 from 2.9 to 9.8. This broad range results from the intermolecular interactions  
364 that the thiol and thiolate states of the cysteine experience inside the protein.  
365 Catalytic cysteines in enzymes like cysteine proteases tend to have nearby  
366 cationic residues, like histidine or asparagine, which lowers their  $pK_a$ 's by  
367 stabilizing the thiolate state of the cysteine [66]. Conversely, the thiolate  
368 state of the cysteine residue will experience repulsive interactions with nearby  
369 anionic residues, raising the  $pK_a$ . Amino acids buried in hydrophobic pockets  
370 of the protein can also have elevated  $pK_a$ 's because they do not experience  
371 stabilizing interactions with water molecules.

372 Calculating the  $pK_a$  of an amino acid side chain in a protein is a long-  
373 standing challenge in computational biophysics. Traditionally, the  $pK_a$  of  
374 an amino acid side chain is estimated based on the relative stability of the  
375 charged and neutral states. Continuum electrostatic models were among the  
376 earliest methods used [67], although the approximations incorporated in their  
377 methodology limit their accuracy. Since this time, these models have been  
378 continually improved, and some methods that make use of an explicit solvent  
379 representation perform well for predicting the  $pK_a$ 's of aspartic and glutamic  
380 acid residues [68, 69].

381 The methods for the prediction of the  $pK_a$  of cysteine residues are less  
382 established. In a recent paper, methods for calculating the  $pK_a$ 's of cysteine  
383 residues in proteins were evaluated for a test set of 18 cysteine  $pK_a$ 's in 12  
384 proteins [41]. Three methods that use an implicit solvent representation were  
385 tested, namely: PROPKA, H++, and MCCE. The root-mean-square devi-  
386 ation (RMSD) of the calculated  $pK_a$ 's with respect to experimental values  
387 were large, with some methods having essentially no predictive power. H++  
388 was the most accurate of the three implicit methods, although the RMSD



389 was still 3.4. A method using an all-atom explicit-solvent model with replica  
390 exchange molecular dynamics thermodynamic integration (REMD-TI) was  
391 more accurate. When used with the CHARMM36 force field, this method was  
392 able to predict the  $pK_a$ 's of cysteine residues in the test set with an RMSD  
393 of 2.4. Plots illustrating the correlation between predicted and experimental  
394 values for these two methods are presented in Figure 9.

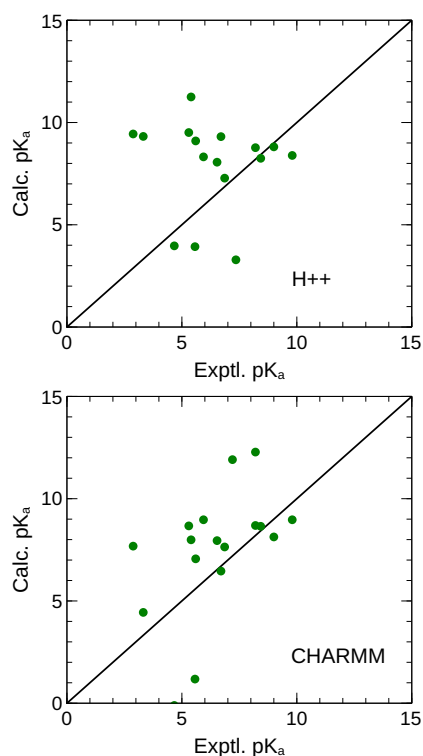


Figure 9: Predictions of cysteine  $pK_a$ 's using implicit-solvent H++ method and an explicit-solvent replica-exchange molecular dynamics free energy calculation method using the CHARMM force field. Adapted from Ref. [41].

395 Although REMD-TI gives reasonably accurate cysteine  $pK_a$ 's, new meth-  
396 ods for calculating the  $pK_a$ 's of cysteines will be needed to allow the reac-  
397 tivity of a cysteine residue to be predicted quantitatively. Improved force  
398 fields and the use of algorithms capable of describing variable protonation  
399 states of other residues within the protein may improve the accuracy of these  
400 methods. Additionally, experimental measurement of more cysteine  $pK_a$ 's in

proteins will allow for a more thorough and comprehensive evaluation of existing  $pK_a$  methods. Of particular importance are the  $pK_a$ 's of noncatalytic residues in protein active sites, which are typically the target of TCIs.

## 5. Quantum Chemical Methodology

The docking and free energy calculation methods described thus far rely on molecular mechanical methods to describe the protein and inhibitor. Typically, these methods do not describe the interactions associated with chemical bonding, so terms like  $\Delta G_{covalent}$  and  $\Delta G^\ddagger$  cannot be calculated by these methods. This has led researchers to employ quantum chemistry to model the mechanisms, kinetics, and structures involved in covalent modification. Density functional theory (DFT) is widely used for modeling biological systems because of its ability to describe large chemical systems with quantitatively accurate energies and structures.

Early models of electrophilic thiol additions were unable to identify the enolate/carbanion intermediates that occur in the canonical mechanism for a thiol-Michael addition. The failure of conventional DFT methods to describe these reactions stems from an issue in contemporary DFT known as delocalization error [70, 71, 72, 73]. DFT calculates inter-electron repulsion in a way that erroneously includes repulsion between an electron and itself, which must be corrected for in an approximate way through the exchange-correlation functional. The result of this effect is a spurious delocalization of electrons to reduce their self-interaction.

Delocalization error is an issue when DFT is used to model thiol additions. The thiolate intermediate features a diffuse, sulfur-centered anion. When some popular DFT functionals are used (e.g., B3LYP or PBE), self-interaction error causes the energy level of the highest occupied molecular orbital (HOMO) to be positive, making the anionic electron formally unbound. When the thiolate is complexed with a Michael acceptor, delocalization error spuriously stabilizes a non-bonded state where electron density is transferred from the HOMO of the thiolate to orbitals of the Michael acceptor. For some electrophiles, this complex is the most stable form and these methods predict that there is no enolate/carbanion intermediate.

One popular method to define the exchange functional in density functional theory calculates the Hartree–Fock exchange energy using the DFT Kohn–Sham orbitals, a technique known as exact exchange. Hybrid DFT

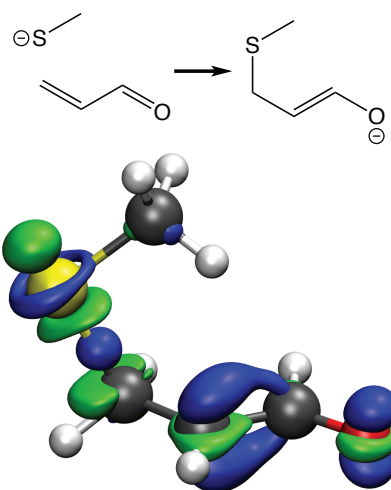


Figure 10: The charge transfer between a thiolate and Michael acceptor calculated using  $\omega$ B97X-D/aug-cc-pVTZ. Charge is transferred from methylthiolate (top) to the acrolein Michael acceptor (bottom). Areas in blue indicate an increase in charge density while areas in green correspond to a decrease in charge density when the two fragments interact. Charge is lost from the thiolate anion and gained in the space between the S-C $_{\alpha}$  sigma bond, the  $\pi$  molecular orbital of the C $_{\alpha}$ -C bond, and the  $p_z$  orbital of the O atom, corresponding to an oxygen-centered anion.

functionals have been developed where part of the exchange energy is calculated by exact exchange. These functionals generally outperform “pure” functionals that do include an exact exchange component.

Issues with delocalization error have led to the development of range-separated DFT functionals, where the exchange-correlation functional uses a large component of exact exchange for long-range inter-electron exchange-correlation. Smith et al. showed that range separated DFT functionals such as  $\omega$ B97X-D predicted a stable thiocarboanion intermediate, while popular methods like B3LYP predicted that this intermediate could not exist as a distinct species (Figure 11). This result was corroborated by highly accurate CCSD(T) calculations [74]. Some hybrid functionals that have a high component of exact exchange globally, such as PBE0 or M06-2X, also predicted a stable carbanion intermediate.

The reaction energies of thiol additions are also sensitive to the DFT functional used. Krenske et al. studied the addition of methyl thiol to  $\alpha,\beta$ -unsaturated ketones [75]. The calculated reaction energies were sensitive to the quantum chemical method used, but the M06-2X and B2PLYP func-

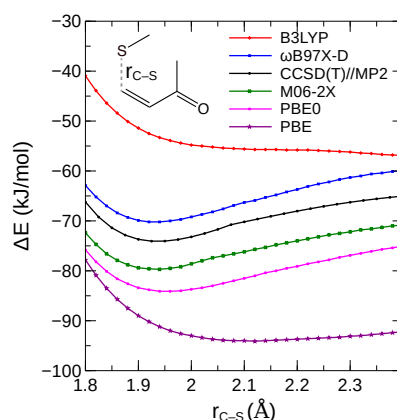


Figure 11: The potential energy surfaces for the addition of methylthiolate to methyl vinyl ketone, calculated using DFT and ab initio methods. The PES for the B3LYP and PBE functionals fail to predict a stable enolate intermediate. High-level ab initio (CCSD(T)), range-separated functions (e.g.,  $\omega$ B97X-D) and hybrid functionals (e.g., PBE0) predict a moderately-stable enolate intermediate with a minimum near  $C_{\beta}$ -S = 1.9 Å.

tionals provided results in close agreement with high-level ab initio results (CBS-QB3). Smith et al. showed that the  $\omega$ B97X-D and PBE0 functionals also provide accurate thiol-addition reaction energies [74].

## 6. Warhead Design

An additional factor in the design of covalent modifiers is the selection of an appropriate functional group for reaction with the target residue of the protein. This warhead is typically an electrophilic group. The type of amino acid undergoing modification is the first design criteria. Covalent modifiers of cysteine residues often feature acrylamides or other electron-deficient alkenes, which can undergo Michael additions to the cysteine residues to form thioether adducts.

Quantum chemistry has been used to model the reaction mechanisms of covalent modification, providing information about the reaction kinetics and thermodynamics for various warheads. For Michael additions to cysteines, a model thiol (e.g., methylthiol) has commonly been used to represent the cysteine residue. The transition state and carbanion intermediate stability can theoretically be used to estimate the rates of reaction ( $k_{inact.}$ ). The Gibbs energy for the net reaction determines whether the addition is spontaneous or non-spontaneous and the degree to which it is reversible.

472 Taunton and coworkers have pursued a line of development of cysteine-  
 473 targeting covalent inhibitors with acrylonitrile warheads with electron donat-  
 474 ing aryl or heteroaryl groups at both the  $\alpha$  and  $\beta$  positions [76]. The most  
 475 effective electrophiles formed a carbanion intermediate with a high proton  
 476 affinity. This warhead was successfully applied to develop a high-affinity  
 477 1,2,4-triazole-activated acrylonitrile covalent modifier that was selective for  
 478 RSK2 kinase.

479 Smith and Rowley implemented an automated workflow to assess the sta-  
 480 bility of the carbanion intermediate and thioether product for the addition  
 481 of a model thiol (methylthiol) to a large set of substituted olefins [77]. All  
 482 combinations of  $-H$ ,  $-CH_3$ ,  $-C(=O)NH(CH_3)$ ,  $-CN$ , and  $-C(=O)OCH_3$   
 483 substituents on an ethene scaffold were evaluated. The lowest energy confor-  
 484 mations of each species were identified by a replica exchange molecular dy-  
 485 namics method [78]. Generally, it was found that substitution of the alkene  
 486 core has a large effect both on the stability of the intermediate and prod-  
 487 ucts, but conventional warheads fell into a narrow range where the addition  
 488 was weakly spontaneous and went through a moderately stable intermediate  
 489 (e.g., 120–160 kJ/mol). This is illustrated in Figure 12, with the approximate  
 490 range of appropriate warheads highlighted in red. Dimethyl fumarate and  
 491 N-methylacrylamide, which are established covalent warheads, are indicated.  
 492 The complete set of calculated reaction energies and intermediate stabilities  
 493 for the full set of warheads are available in the supporting information of  
 494 Ref. 77.

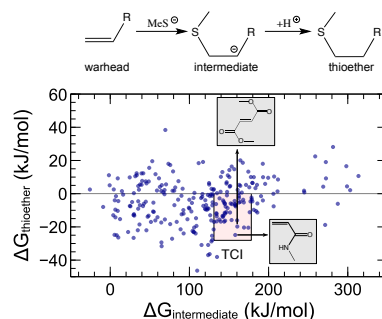


Figure 12: The calculated stability of the carbanion intermediate vs. the stability of the thioether product for the full data set of model thiol additions from Smith and Rowley [77]. The region of potential TCI warheads is highlighted, where the thiol undergoes a weakly exergonic addition ( $\Delta G_{thioether} < 0$ ) through a moderately-stable carbanion intermediate ( $130 \text{ kJ/mol} < \Delta G_{intermediate} < 180 \text{ kJ/mol}$ ).

495 The calculated reaction energies of warheads used in successful TCIs are  
 496 weakly exergonic, which makes these reactions reversible. This allows them to  
 497 dissociate from non-targeted thiols should they react with an off-target thiol  
 498 in the cell prior to reaching their target. This is consistent with an emerging  
 499 principle of TCI design, which is that the warhead should only be moderately  
 500 reactive in order to avoid promiscuous modification [79, 80, 20]. Because  
 501 thiol additions to warheads like acrylamides are reversible, modification of  
 502 an off-target protein can be reversed. The moderate rate of reaction due to a  
 503 moderately stable enolate intermediate favors the formation of the covalent  
 504 bond only after the inhibitor has complexed to its target through selective  
 505 non-covalent interactions. Of the hundreds of putative warheads evaluated in  
 506 this study, only a small number have the appropriate thiol-addition kinetics  
 507 and thermochemistry to serve as a therapeutic TCI.

508 Krenske et al. studied the addition of methyl thiol to  $\alpha$ ,  $\beta$ -unsaturated  
 509 ketones [75].  $\alpha$ -methyl,  $\beta$ -methyl, and  $\alpha$ -phenyl ketones were found to be more  
 510 readily reversible than the unsubstituted vinyl ketone. A subsequent study by  
 511 Krenske et al. used DFT calculations to study the Michael acceptor warheads  
 512 with aryl groups at the  $\alpha$ -position and electron withdrawing groups at the  
 513  $\beta$ -position [81]. These calculations were consistent with the experimental  
 514 observation by Taunton et al., who observed that electrophiles with two  
 515 electron withdrawing groups at the  $\alpha$ -position (e.g., amide and cyano) and an  
 516 aryl at the  $\beta$ -position yielded a warhead that reacted covalently but reversibly  
 517 with thiols [20].

518 Zhao and coworkers calculated the potential energy surfaces for the addi-  
 519 tion of a model thiol to an  $\alpha$ ,  $\beta$ -unsaturated aldehyde in a range of dielectric  
 520 environments [43]. The barrier to a direct 1,2 addition and ammonia-assisted  
 521 addition was higher in low-dielectric environments, suggesting that the rates  
 522 of covalent modification through these mechanisms will be lower in cysteine  
 523 residues buried in hydrophobic binding pockets. It should be noted these  
 524 mechanisms are distinct from the canonical Michael addition mechanism,  
 525 where the reaction proceeds through a thiolate and carbanion intermediate.  
 526 These calculations used the B3LYP exchange-correlation functional, which  
 527 tends to underestimate the stability of carbanion intermediates and thioether  
 528 products [74].

## 529 7. QM/MM Models of Covalent Modification

530 Studies of covalent modification using model reactants in the gas phase  
 531 or using a continuum solvent model do not provide a rigorous description of  
 532 how the protein environment affects the reaction between the protein and  
 533 the inhibitor. Paasche et al. found that continuum solvent models provided  
 534 limited success in describing the cysteine–histidine proton transfer reactions  
 535 associated with cysteine protease function [82]. Describing the full enzyme,  
 536 inhibitor, and solvent using a quantum mechanical model would be pro-  
 537 hibitively computationally demanding, so it is not practical to apply these  
 538 methods naively to model the covalent modification of a protein.

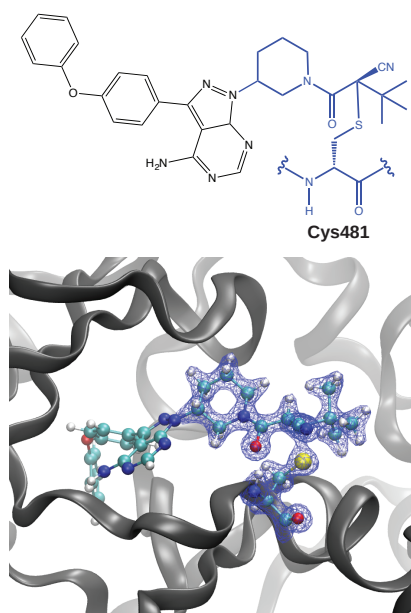


Figure 13: An example QM/MM model of Bruton's tyrosine kinase in complex with a covalent modifier (Ref. 20, PDB ID: 4YHF). The covalently-modified Cys481 residue and the cyanoacrylamide warhead define the QM region. The calculated electron density of the QM region is represented by the blue mesh. The remainder of the protein (gray) and inhibitor comprise the MM region.

539 Quantum mechanics/molecular mechanics (QM/MM) methods allow for  
 540 a critical component of a chemical system to be described using a quantum  
 541 mechanical model, while the rest of the system is represented using a molec-  
 542 ular mechanical model (Figure 13). As the size of the QM region is reduced

to a relatively small size, the computational expense of these QM/MM calculations is tractable. This is well-suited for modeling chemical reactions involving proteins, like enzymatic reaction mechanisms, where the chemical reaction only directly involves a small number of atoms, but the rest of system provides an essential environment. Analogously, the covalent modification of proteins can also be described using a QM/MM model, where the reactive warhead of the inhibitor and the residue being modified are described using QM, while the balance of the system, such as the solvent and the rest of the protein are described using an MM model. If needed, additional sections of the inhibitor and protein can be included in the QM region. QM/MM methods are now available in codes such as Gaussian [83], CHARMM [84], Amber [85], NAMD [86], and ChemShell [87, 88].

One example of QM/MM modeling of covalent modification probed the mechanisms involved in the covalent modification of Ser530 of cyclooxygenase by aspirin. Tosco and Lazzarato [89] constructed a QM/MM model where an aspirin molecule and the nearby amino acid residues in the enzyme active site (e.g., Ser530, Tyr348, and Tyr385) were modeled using semiempirical SCC-DFTB QM method and the balance of the system was modeled using the CHARMM force field. The aim was to propose a putative reaction mechanism for the irreversible inactivation of cyclooxygenase by aspirin. The results obtained suggests that acetylation of Ser530 in cyclooxygenase by aspirin occurs under intramolecular general base catalysis conditions, where the vicinal carboxylate group of aspirin abstracts a proton from the hydroxy group of Ser530 in cyclooxygenase, followed by a nucleophilic attack by the  $O_\gamma$  of Ser530 on the acetyl carbonyl carbon of aspirin. This forms an anionic tetrahedral intermediate, which is stabilized by Tyr385.

Tóth et al. [90] also reported a QM/MM study of the reaction mechanism, transition state, and potential energy surface of the inhibition reaction of cyclooxygenase by aspirin. In their approach, static ONIOM-type QM/MM methods were used, where the HF, B3LYP, MP2, and B97-D methods were used to describe the QM region, which was comprised of the aspirin molecule and surrounding amino acids. The authors concluded that the transesterification reaction of aspirin and cyclooxygenase occurs through a concerted mechanism.

QM/MM methods have also been employed in studying the mechanism of enzyme inhibition in peptide cleaving enzymes, such as cysteine proteases [91, 92]. A wide range of warheads will react readily with the acidic catalytic cysteine, so covalent-modifiers have frequently been used to inhibit these



581 targets. QM/MM studies have examined the inhibition of cysteine proteases  
582 by epoxides [93], aziridines [94], peptidyl aldehydes [95], vinyl sulfones [96],  
583 and nitroalkene-based inhibitors [97] of cysteine proteases, among others. It  
584 should be noted that some of these studies used DFT methods (e.g., B3LYP)  
585 that underestimate the stability of the enolate intermediate [77].

586 Engels and coworkers have published a series of computational studies  
587 [92, 94, 98, 99, 100] that explore the factors governing the kinetics, re-  
588 giospecificity and stereoselectivity of epoxide- and aziridine-based inhibitors  
589 of cysteine proteases. QM/MM and molecular dynamics (MD) methods were  
590 used to investigate basic mechanistic principles and inhibition processes of  
591 these enzymatic reactions. Hydrogen bonds between the inhibitor and other  
592 residues in the active site were found to affect the reaction mechanism sig-  
593 nificantly, demonstrating that the explicit representation of the active site  
594 was necessary to describe the reaction mechanism. These studies aided the  
595 design and synthesis of new, potent inhibitors of this family of enzymes  
596 [94, 101, 102].

597 Schirmeister et al. [103] developed QM/MM-based workflow for the devel-  
598 opment of covalent inhibitors. Using an existing protein-inhibitor structure,  
599 the substituents on the warhead are systematically varied. A QM/MM model  
600 of the protein-inhibitor complex is used to calculate the potential energy sur-  
601 face of the covalent modification, which provided the activation energy and  
602 reaction energy. The docking programs FlexX and DOCKTITE were used  
603 to identify variants on the drug scaffold that would improve the non-covalent  
604 component of the binding energy. The covalent competence of this new war-  
605 head were tested by a second round of QM/MM calculations. This workflow  
606 was used to develop novel covalent vinyl sulfone-based inhibitors of rhode-  
607 sian, a parasite protease belonging to the papain family of cysteine proteases.  
608 The halogenated warhead designed by this procedure was predicted to be a  
609 reversible covalent modifier, which was confirmed experimentally.

610 Another QM/MM workflow for the design of covalent inhibitors was re-  
611 ported by Fanfrlik et al. [96], which uses a QM-based scoring function based  
612 on a hybrid QM/semi-empirical QM model to describe the process of covalent  
613 binding in protein–ligand complexes. The performance of the algorithm was  
614 evaluated on a series of vinyl sulfone-based inhibitors of *S. mansoni* cathep-  
615 sin B1. The calculated Gibbs energy difference between the non-covalently-  
616 bound state and the covalently-bound state was found to correlate to the log  
617 of the experimental  $IC_{50}$  with a coefficient of determination of 0.69.

618 QM/MM modeling has the potential to play a significant role in under-

standing and predicting the mechanisms, kinetics, and thermodynamics of covalent modification. More accurate QM methods, improved algorithms to interface the QM and MM regions, and more extensive configurational sampling will be needed to make these methods quantitatively accurate. In combination with other simulation methods to calculate the non-covalent binding and deprotonation steps, QM/MM methods can be used to calculate the kinetic and thermodynamics terms of covalent modification rigorously. Ultimately, the integration of these methods will make it possible to model the action of covalent modifier drugs in a comprehensive way through the calculation of  $\Delta G_{non-covalent}$  and  $\Delta G^\ddagger$ .

## 8. Conclusions

Computational methods for modeling the covalent modification of proteins have developed rapidly over the last 10 years. Docking programs such as AutoDock, Glide, and MOE now include functionality to find poses of docked covalent modifiers. The design of reactive warheads has been aided by quantum chemical modeling of model reactions. One of the most promising areas of this field is the use of computer modeling to examine the reaction mechanisms of covalent modification;  $pK_a$  calculations can be used to determine the reactivity of targeted residues and QM/MM models can be used to elucidate the reaction mechanism, activation energy, and covalent binding energy. With further developments in computing power and more accurate computational methods, these methods may eventually allow the estimation of rates of inactivation and the covalent component of the binding energy. The maturation of these methods will allow computer modeling to contribute to the development of covalent-modifier drugs to the same degree that they have contributed to the development of non-covalent drugs.

## 9. Acknowledgements

The authors thank NSERC of Canada for funding through the Discovery Grant program (Application 418505-2012). EAW thanks the School of Graduate Studies at Memorial University for a graduate fellowship. EAW also thanks ACENET for an Advanced Research Computing Fellowship. Computational resources were provided by Compute Canada (RAPI: djc-615-ab) through the Calcul Quebec, Westgrid, and ACENET consortia. We thank Schrödinger Inc. for a temporary license of Maestro/Glide. We thank Professor Erin Johnson for assistance with the charge transfer figure.

## 10. References

- [1] I. D. Kuntz, K. Chen, K. A. Sharp, P. A. Kollman, The maximal affinity of ligands, *Proc. Natl. Acad. Sci. U.S.A.* 96 (1999) 9997–10002.
- [2] P. A. Jackson, J. C. Widen, D. A. Harki, K. M. Brummond, Covalent modifiers: A chemical perspective on the reactivity of  $\alpha$ -unsaturated carbonyls with thiols via hetero-michael addition reactions, *J. Med. Chem.* 60 (2017) 839–885.
- [3] M. H. Potashman, M. E. Duggan, Covalent Modifiers: An Orthogonal Approach to Drug Design, *J. Med. Chem.* 52 (2009) 1231–1246.
- [4] J. Singh, R. C. Petter, T. A. Baillie, A. Whitty, The resurgence of covalent drugs, *Nat. Rev. Drug Discov.* 10 (2011) 307–317.
- [5] A. S. Kalgutkar, D. K. Dalvie, Drug discovery for a new generation of covalent drugs, *Expert Opin. Drug Discov.* 7 (2012) 561–581.
- [6] A. J. Wilson, J. K. Kerns, J. F. Callahan, C. J. Moody, Keep calm, and carry on covalently, *J. Med. Chem.* 56 (2013) 7463–7476.
- [7] R. A. Bauer, Covalent inhibitors in drug discovery: from accidental discoveries to avoided liabilities and designed therapies, *Drug Discov. Today* 20 (2015) 1061–1073.
- [8] T. A. Baillie, Targeted covalent inhibitors for drug design, *Angew. Chem. Int. Ed.* 55 (2016) 13408–13421.
- [9] J. C. Powers, J. L. Asgian, Ö. D. Ekici, K. E. James, Irreversible inhibitors of serine, cysteine, and threonine proteases, *Chem. Rev.* 102 (2002) 4639–4750.
- [10] A. Miseta, P. Csutora, Relationship between the occurrence of cysteine in proteins and the complexity of organisms, *Mol. Biol. Evol.* 17 (2000) 1232–1239.
- [11] C. Jöst, C. Nitsche, T. Scholz, L. Roux, C. D. Klein, Promiscuity and selectivity in covalent enzyme inhibition: A systematic study of electrophilic fragments, *J. Med. Chem.* 57 (2014) 7590–7599.

- 683 [12] K. M. Backus, B. E. Correia, K. M. Lum, S. Forli, B. D. Horning,  
684 G. E. González-Páez, S. Chatterjee, B. R. Lanning, J. R. Teijaro, A. J.  
685 Olson, D. W. Wolan, B. F. Cravatt, Proteome-wide covalent ligand  
686 discovery in native biological systems, *Nature* 534 (2016) 570–574.
- 687 [13] C. G. Parker, A. Galmozzi, Y. Wang, B. E. Correia, K. Sasaki, C. M.  
688 Joslyn, A. S. Kim, C. L. Cavallaro, R. M. Lawrence, S. R. Johnson,  
689 I. Narvaiza, E. Saez, B. F. Cravatt, Ligand and target discovery by  
690 fragment-based screening in human cells, *Cell* 168 (2017) 527–541.e29.
- 691 [14] D. S. Johnson, E. Weerapana, B. F. Cravatt, Strategies for discovering  
692 and derisking covalent, irreversible enzyme inhibitors, *Future Med.*  
693 *Chem.* 2 (2010) 949–964.
- 694 [15] M. H. Johansson, Reversible michael additions: Covalent inhibitors  
695 and prodrugs, *Mini-Rev. Med. Chem.* 12 (2012) 1330–1344.
- 696 [16] H.-J. Woo, B. Roux, Calculation of absolute protein–ligand binding  
697 free energy from computer simulations, *Proc. Natl. Acad. Sci. U.S.A.*  
698 102 (2005) 6825–6830.
- 699 [17] Z. D. Nagel, J. P. Klinman, A 21st century revisionist’s view at a  
700 turning point in enzymology, *Nat. Chem. Biol.* 5 (2009) 543–550.
- 701 [18] M. H. Olsson, J. Mavri, A. Warshel, Transition state theory can be used  
702 in studies of enzyme catalysis: lessons from simulations of tunnelling  
703 and dynamical effects in lipoxygenase and other systems, *Philos. Trans.*  
704 *R. Soc., B* 361 (2006) 1417–1432.
- 705 [19] R. A. Copeland, D. L. Pompliano, T. D. Meek, Drug-target residence  
706 time and its implications for lead optimization, *Nat. Rev. Drug Discov.*  
707 5 (2006) 730–739.
- 708 [20] J. M. Bradshaw, J. M. McFarland, V. O. Paavilainen, A. Bisconte,  
709 D. Tam, V. T. Phan, S. Romanov, D. Finkle, J. Shu, V. Patel, T. Ton,  
710 X. Li, D. G. Loughhead, P. A. Nunn, D. E. Karr, M. E. Gerritsen,  
711 J. O. Funk, T. D. Owens, E. Verner, K. A. Brameld, R. J. Hill, D. M.  
712 Goldstein, J. Taunton, Prolonged and tunable residence time using  
713 reversible covalent kinase inhibitors, *Nat. Chem. Biol.* 11 (2015) 525–  
714 531.

- 715 [21] R. A. Copeland, The drug-target residence time model: a 10-year  
716 retrospective, *Nat Rev Drug Discov* 15 (2016) 87–95. Perspectives.
- 717 [22] R. Mannhold, G. I. Poda, C. Ostermann, I. V. Tetko, Calculation of  
718 molecular lipophilicity: State-of-the-art and comparison of logp meth-  
719 ods on more than 96,000 compounds, *J. Pharm. Sci.* 98 (2009) 861–893.
- 720 [23] E. Awoonor-Williams, C. N. Rowley, Molecular simulation of nonfa-  
721 cilitated membrane permeation, *Biochim. Biophys. Acta, Biomembr.*  
722 1858 (2016) 1672–1687.
- 723 [24] C. T. Lee, J. Comer, C. Herndon, N. Leung, A. Pavlova, R. V. Swift,  
724 C. Tung, C. N. Rowley, R. E. Amaro, C. Chipot, Y. Wang, J. C. Gum-  
725 bart, Simulation-based approaches for determining membrane perme-  
726 ability of small compounds, *J. Chem. Inf. Model.* 56 (2016) 721–733.
- 727 [25] E. Yuriev, M. Agostino, P. A. Ramsland, Challenges and advances  
728 in computational docking: 2009 in review, *J. Mol. Recogn.* 24 (2011)  
729 149–164.
- 730 [26] T. Cheng, Q. Li, Z. Zhou, Y. Wang, S. H. Bryant, Structure-based  
731 virtual screening for drug discovery: a problem-centric review, *AAPS*  
732 *J.* 14 (2012) 133–141.
- 733 [27] G. Sliwoski, S. Kothiwale, J. Meiler, E. W. Lowe, Computational  
734 methods in drug discovery, *Pharmacol. Rev.* 66 (2013) 334–395.
- 735 [28] J. Wang, Y. Deng, B. Roux, Absolute binding free energy calculations  
736 using molecular dynamics simulations with restraining potentials, *Bio-*  
737 *phys J.* 91 (2006) 2798–2814.
- 738 [29] J. Michel, J. W. Essex, Prediction of protein–ligand binding affinity  
739 by free energy simulations: assumptions, pitfalls and expectations, *J.*  
740 *Comput. Aided Mol. Des.* 24 (2010) 639–658.
- 741 [30] J. D. Chodera, D. L. Mobley, M. R. Shirts, R. W. Dixon, K. Bran-  
742 son, V. S. Pande, Alchemical free energy methods for drug discovery:  
743 progress and challenges, *Curr. Opin. Struct. Biol.* 21 (2011) 150–160.
- 744 [31] L. Wang, Y. Wu, Y. Deng, B. Kim, L. Pierce, G. Krilov, D. Lupyan,  
745 S. Robinson, M. K. Dahlgren, J. Greenwood, D. L. Romero, C. Masse,

- 746 J. L. Knight, T. Steinbrecher, T. Beuming, W. Damm, E. Harder,  
747 W. Sherman, M. Brewer, R. Wester, M. Murcko, L. Frye, R. Farid,  
748 T. Lin, D. L. Mobley, W. L. Jorgensen, B. J. Berne, R. A. Friesner,  
749 R. Abel, Accurate and reliable prediction of relative ligand binding  
750 potency in prospective drug discovery by way of a modern free-energy  
751 calculation protocol and force field, *J. Am. Chem. Soc.* 137 (2015)  
752 2695–2703.
- 753 [32] H. M. Kumalo, S. Bhakat, M. E. S. Soliman, Theory and applications  
754 of covalent docking in drug discovery: Merits and pitfalls, *Molecules*  
755 20 (2015) 1984–2000.
- 756 [33] H. M. Berman, J. Westbrook, Z. Feng, G. Gilliland, T. N. Bhat,  
757 H. Weissig, I. N. Shindyalov, P. E. Bourne, The protein data bank,  
758 *Nucleic Acids Res.* 28 (2000) 235.
- 759 [34] M. I. Davis, J. P. Hunt, S. Herrgard, P. Ciceri, L. M. Wodicka, G. Pal-  
760 lares, M. Hocker, D. K. Treiber, P. P. Zarrinkar, Comprehensive analy-  
761 sis of kinase inhibitor selectivity, *Nat. Biotechnol.* 29 (2011) 1046–1051.
- 762 [35] T. Barf, A. Kaptein, Irreversible protein kinase inhibitors: Balancing  
763 the benefits and risks, *J. Med. Chem.* 55 (2012) 6243–6262.
- 764 [36] Q. Liu, Y. Sabnis, Z. Zhao, T. Zhang, S. Buhrlage, L. Jones, N. Gray,  
765 Developing irreversible inhibitors of the protein kinase cysteinome,  
766 *Chem. Biol.* 20 (2013) 146–159.
- 767 [37] M. S. Cohen, C. Zhang, K. M. Shokat, J. Taunton, Structural  
768 bioinformatics-based design of selective, irreversible kinase inhibitors,  
769 *Science* 308 (2005) 1318–1321.
- 770 [38] J. Zhang, P. L. Yang, N. S. Gray, Targeting cancer with small molecule  
771 kinase inhibitors, *Nat. Rev. Cancer* 9 (2009) 28–39.
- 772 [39] E. Leproult, S. Barluenga, D. Moras, J.-M. Wurtz, N. Winssinger, Cys-  
773 teine mapping in conformationally distinct kinase nucleotide binding  
774 sites: Application to the design of selective covalent inhibitors, *J. Med.*  
775 *Chem.* 54 (2011) 1347–1355.
- 776 [40] S. Wu, H. L. (Howard), H. Wang, W. Zhao, Q. Hu, Y. Yang, Cys-  
777 teinome: The first comprehensive database for proteins with targetable

- 778 cysteine and their covalent inhibitors, *Biochem. Biophys. Res. Commun.* 478 (2016) 1268 – 1273.  
779
- 780 [41] E. Awoonor-Williams, C. N. Rowley, Evaluation of methods for the  
781 calculation of the pKa of cysteine residues in proteins, *J. Chem. Theory*  
782 *Comput.* 12 (2016) 4662–4673.
- 783 [42] Z. Zhao, L. Xie, L. Xie, P. E. Bourne, Delineation of polypharmacology  
784 across the human structural kinome using a functional site interaction  
785 fingerprint approach, *J. Med. Chem.* 59 (2016) 4326–4341.
- 786 [43] Z. Zhao, Q. Liu, S. Bliven, L. Xie, P. E. Bourne, Determining cysteines  
787 available for covalent inhibition across the human kinome, *J. Med.*  
788 *Chem.* 60 (2017) 2879–2889.
- 789 [44] X. Fradera, J. Kaur, J. Mestres, Unsupervised guided docking of covalently bound ligands, *J. Comput. Aided Mol. Des.* 18 (2004) 635–650.  
790
- 791 [45] N. Moitessier, J. Pottel, E. Therrien, P. Englebienne, Z. Liu,  
792 A. Tomberg, C. R. Corbeil, Medicinal chemistry projects requiring  
793 imaginative structure-based drug design methods, *Acc. Chem. Res.* 49  
794 (2016) 1646–1657.
- 795 [46] N. London, R. M. Miller, S. Krishnan, K. Uchida, J. J. Irwin, O. Eidam,  
796 L. Gibold, R. Bonnet, P. Cimermančič, B. K. Shoichet, J. Taunton,  
797 Covalent docking of large libraries for the discovery of chemical probes,  
798 *Nat. Chem. Biol.* 10 (2014) 1066–1072.
- 799 [47] K. Zhu, K. W. Borrelli, J. R. Greenwood, T. Day, R. Abel, R. S. Farid,  
800 E. Harder, Docking covalent inhibitors: A parameter free approach to  
801 pose prediction and scoring, *J. Chem. Inf. Model.* 54 (2014) 1932–1940.
- 802 [48] D. Toledo Warshaviak, G. Golan, K. W. Borrelli, K. Zhu, O. Kalid,  
803 Structure-based virtual screening approach for discovery of covalently  
804 bound ligands, *J. Chem. Inf. Model.* 54 (2014) 1941–1950.
- 805 [49] G. Bianco, S. Forli, D. S. Goodsell, A. J. Olson, Covalent docking  
806 using autodock: Two-point attractor and flexible side chain methods,  
807 *Protein Sci.* 25 (2016) 295–301.



- 808 [50] C. Scholz, S. Knorr, K. Hamacher, B. Schmidt, Docktite – a highly  
809 versatile step-by-step workflow for covalent docking and virtual screen-  
810 ing in the molecular operating environment, *J. Chem. Inf. Model.* 55  
811 (2015) 398–406.
- 812 [51] C. R. Corbeil, P. Englebienne, N. Moitessier, Docking ligands into  
813 flexible and solvated macromolecules. 1. development and validation of  
814 FITTED 1.0, *J. Chem. Inf. Model.* 47 (2007) 435–449.
- 815 [52] C. R. Corbeil, N. Moitessier, Docking ligands into flexible and solvated  
816 macromolecules. 3. impact of input ligand conformation, protein flex-  
817 ibility, and water molecules on the accuracy of docking programs, *J.*  
818 *Chem. Inf. Model.* 49 (2009) 997–1009.
- 819 [53] J. Lawandi, S. Toumieux, V. Seyer, P. Campbell, S. Thielges,  
820 L. Juillerat-Jeanneret, N. Moitessier, Constrained peptidomimetics re-  
821 veal detailed geometric requirements of covalent prolyl oligopeptidase  
822 inhibitors, *J. Med. Chem.* 52 (2009) 6672–6684.
- 823 [54] S. De Cesco, S. Deslandes, E. Therrien, D. Levan, M. Cueto,  
824 R. Schmidt, L.-D. Cantin, A. Mittermaier, L. Juillerat-Jeanneret,  
825 N. Moitessier, Virtual screening and computational optimization for  
826 the discovery of covalent prolyl oligopeptidase inhibitors with activity  
827 in human cells, *J. Med. Chem.* 55 (2012) 6306–6315.
- 828 [55] G. Mariaule, S. De Cesco, F. Airaghi, J. Kurian, P. Schiavini, S. Roche-  
829 leau, I. Huskić, K. Auclair, A. Mittermaier, N. Moitessier, 3-oxo-  
830 hexahydro-1h-isoindole-4-carboxylic acid as a drug chiral bicyclic scaf-  
831 fold: Structure-based design and preparation of conformationally con-  
832 strained covalent and noncovalent prolyl oligopeptidase inhibitors, *J.*  
833 *Med. Chem.* 59 (2016) 4221–4234.
- 834 [56] A. Del Rio, M. Sgobba, M. D. Parenti, G. Degliesposti, R. Forestiero,  
835 C. Percivalle, P. F. Conte, M. Freccero, G. Rastelli, A computational  
836 workflow for the design of irreversible inhibitors of protein kinases, *J*  
837 *Comput. Aided Mol. Des.* 24 (2010) 183–194.
- 838 [57] X. Ouyang, S. Zhou, C. T. T. Su, Z. Ge, R. Li, C. K. Kwoh, Co-  
839 valentdock: Automated covalent docking with parameterized covalent



- linkage energy estimation and molecular geometry constraints, *J. Comput. Chem.* 34 (2013) 326–336.
- [58] X. Ouyang, S. Zhou, Z. Ge, R. Li, C. K. Kwok, Covalentdock cloud: A web server for automated covalent docking, *Nucleic Acids Res.* 41 (2013) W329.
- [59] G. Bianco, S. Forli, D. S. Goodsell, A. J. Olson, Covalent docking using autodock: Two-point attractor and flexible side chain methods, *Protein Sci.* 25 (2016) 295–301.
- [60] M. P. Jacobson, R. A. Friesner, Z. Xiang, B. Honig, On the role of the crystal environment in determining protein side-chain conformations, *J. Mol. Biol.* 320 (2002) 597–608.
- [61] M. P. Jacobson, D. L. Pincus, C. S. Rapp, T. J. Day, B. Honig, D. E. Shaw, R. A. Friesner, A hierarchical approach to all-atom protein loop prediction, *Proteins: Struct., Funct., Bioinf.* 55 (2004) 351–367.
- [62] Y. Ai, L. Yu, X. Tan, X. Chai, S. Liu, Discovery of covalent ligands via noncovalent docking by dissecting covalent docking based on a “steric-clashes alleviating receptor (SCAR)” strategy, *J. Chem. Inf. Model.* 56 (2016) 1563–1575.
- [63] Molecular Operating Environment (MOE) 2013.08 Chemical Computing Group inc. 1010 Sherbooke St. West Suite #910 Montreal Q, Canada H3A 2R7, 2017.
- [64] T. Schirmeister, J. Schmitz, S. Jung, T. Schmenger, R. L. Krauth-Siegel, M. Gütschow, Evaluation of dipeptide nitriles as inhibitors of rhodesain, a major cysteine protease of *Trypanosoma brucei*, *Bioorg. Med. Chem. Lett.* 27 (2017) 45–50.
- [65] R. L. Thurkill, G. R. Grimsley, J. M. Scholtz, C. N. Pace, pK values of the ionizable groups of proteins, *Protein Sci.* 15 (2006) 1214–1218.
- [66] S. Pinitglang, A. B. Watts, M. Patel, J. D. Reid, M. A. Noble, S. Gul, A. Bokth, A. Naeem, H. Patel, E. W. Thomas, S. K. Sreedharan, C. Verma, K. Brocklehurst, A classical enzyme active center motif lacks catalytic competence until modulated electrostatically, *Biochemistry* 36 (1997) 9968–9982.

- 872 [67] D. Bashford, M. Karplus, pKa's of ionizable groups in proteins: Atomic  
873 detail from a continuum electrostatic model, *Biochemistry* 29 (1990)  
874 10219–10225.
- 875 [68] T. Simonson, J. Carlsson, D. A. Case, Proton binding to proteins: pka  
876 calculations with explicit and implicit solvent models, *J. Am. Chem.*  
877 *Soc.* 126 (2004) 4167–4180.
- 878 [69] E. Alexov, E. L. Mehler, N. Baker, A. M. Baptista, Y. Huang, F. Mil-  
879 letti, J. Erik Nielsen, D. Farrell, T. Carstensen, M. H. M. Olsson, J. K.  
880 Shen, J. Warwicker, S. Williams, J. M. Word, Progress in the predic-  
881 tion of pKa values in proteins, *Proteins: Struct., Funct., Bioinf.* 79  
882 (2011) 3260–3275.
- 883 [70] E. R. Johnson, P. Mori-Sánchez, A. J. Cohen, W. Yang, Delocalization  
884 errors in density functionals and implications for main-group thermo-  
885 chemistry, *J. Chem. Phys.* 129 (2008) 204112.
- 886 [71] A. J. Cohen, P. Mori-Sánchez, W. Yang, Insights into current limita-  
887 tions of density functional theory, *Science* 321 (2008) 792–794.
- 888 [72] J. Autschbach, M. Srebro, Delocalization error and functional tuning  
889 in kohnsham calculations of molecular properties, *Acc. Chem. Res.* 47  
890 (2014) 2592–2602.
- 891 [73] A. Wasserman, J. Nafziger, K. Jiang, M.-C. Kim, E. Sim, K. Burke,  
892 The importance of being self-consistent, *Annu. Rev. Phys. Chem.*  
893 (2017).
- 894 [74] J. M. Smith, Y. Jami Alahmadi, C. N. Rowley, Range-separated dft  
895 functionals are necessary to model thio-Michael additions, *J. Chem.*  
896 *Theory Comput.* 9 (2013) 4860–4865.
- 897 [75] E. H. Krenske, R. C. Petter, Z. Zhu, K. N. Houk, Transition states  
898 and energetics of nucleophilic additions of thiols to substituted  $\alpha$ -  
899 unsaturated ketones: Substituent effects involve enone stabilization,  
900 product branching, and solvation, *J. Org. Chem.* 76 (2011) 5074–5081.
- 901 [76] S. Krishnan, R. M. Miller, B. Tian, R. D. Mullins, M. P. Jacobson,  
902 J. Taunton, Design of reversible, cysteine-targeted michael acceptors

- 903 guided by kinetic and computational analysis, *J. Am. Chem. Soc.* 136  
904 (2014) 12624–12630.
- 905 [77] J. M. Smith, C. N. Rowley, Automated computational screening of the  
906 thiol reactivity of substituted alkenes, *J. Comput.-Aided Mol. Des.* 29  
907 (2015) 725–735.
- 908 [78] K. Gaalswyk, C. N. Rowley, An explicit-solvent conformation search  
909 method using open software., *PeerJ* 4 (2016) e2088.
- 910 [79] I. M. Serafimova, M. A. Pufall, S. Krishnan, K. Duda, M. S. Co-  
911 hen, R. L. Maglathlin, J. M. McFarland, R. M. Miller, M. Frödin,  
912 J. Taunton, Reversible targeting of noncatalytic cysteines with chemi-  
913 cally tuned electrophiles, *Nat. Chem. Biol.* 8 (2012) 471–476.
- 914 [80] P. A. Schwartz, P. Kuzmic, J. Solowiej, S. Bergqvist, B. Bolanos, C. Al-  
915 maden, A. Nagata, K. Ryan, J. Feng, D. Dalvie, J. C. Kath, M. Xu,  
916 R. Wani, B. W. Murray, Covalent EGFR inhibitor analysis reveals im-  
917 portance of reversible interactions to potency and mechanisms of drug  
918 resistance, *Proc. Natl. Acad. Sci. USA* 111 (2014) 173–178.
- 919 [81] E. H. Krenske, R. C. Petter, K. N. Houk, Kinetics and thermody-  
920 namics of reversible thiol additions to mono- and deactivated Michael  
921 acceptors: Implications for the design of drugs that bind covalently to  
922 cysteines, *J. Org. Chem.* 81 (2016) 11726–11733.
- 923 [82] A. Paasche, T. Schirmeister, B. Engels, Benchmark study for the  
924 cysteine–histidine proton transfer reaction in a protein environment:  
925 Gas phase, COSMO, QM/MM approaches, *J. Chem. Theory Comput.*  
926 9 (2013) 1765–1777.
- 927 [83] M. J. Frisch, G. W. Trucks, H. B. Schlegel, G. E. Scuseria, M. A. Robb,  
928 J. R. Cheeseman, G. Scalmani, V. Barone, G. A. Petersson, H. Nakat-  
929 suji, X. Li, M. Caricato, A. V. Marenich, J. Bloino, B. G. Janesko,  
930 R. Gomperts, B. Mennucci, H. P. Hratchian, J. V. Ortiz, A. F. Iz-  
931 maylov, J. L. Sonnenberg, D. Williams-Young, F. Ding, F. Lipparini,  
932 F. Egidi, J. Goings, B. Peng, A. Petrone, T. Henderson, D. Ranasinghe,  
933 V. G. Zakrzewski, J. Gao, N. Rega, G. Zheng, W. Liang, M. Hada,  
934 M. Ehara, K. Toyota, R. Fukuda, J. Hasegawa, M. Ishida, T. Naka-  
935 jima, Y. Honda, O. Kitao, H. Nakai, T. Vreven, K. Throssell, J. A.

- 936 Montgomery, Jr., J. E. Peralta, F. Ogliaro, M. J. Bearpark, J. J.  
937 Heyd, E. N. Brothers, K. N. Kudin, V. N. Staroverov, T. A. Keith,  
938 R. Kobayashi, J. Normand, K. Raghavachari, A. P. Rendell, J. C. Bu-  
939 rant, S. S. Iyengar, J. Tomasi, M. Cossi, J. M. Millam, M. Klene,  
940 C. Adamo, R. Cammi, J. W. Ochterski, R. L. Martin, K. Morokuma,  
941 O. Farkas, J. B. Foresman, D. J. Fox, Gaussian16 Revision A.03, 2016.  
942 Gaussian Inc. Wallingford CT.
- 943 [84] S. Riahi, C. N. Rowley, The CHARMM–TURBOMOLE interface for  
944 efficient and accurate QM/MM molecular dynamics, free energies, and  
945 excited state properties, *J. Comput. Chem.* 35 (2014) 2076–2086.
- 946 [85] R. C. Walker, M. F. Crowley, D. A. Case, The implementation of a  
947 fast and accurate QM/MM potential method in Amber, *J. Comput.*  
948 *Chem.* 29 (2008) 1019–1031.
- 949 [86] J. C. Phillips, R. Braun, W. Wang, J. Gumbart, E. Tajkhorshid,  
950 E. Villa, C. Chipot, R. D. Skeel, L. Kale, K. Schulten, Scalable molec-  
951 ular dynamics with namd, *J. Comput. Chem.* 26 (2005) 1781–1802.
- 952 [87] P. Sherwood, A. H. de Vries, M. F. Guest, G. Schreckenbach, C. R. A.  
953 Catlow, S. A. French, A. A. Sokol, S. T. Bromley, W. Thiel, A. J.  
954 Turner, et al., QUASI: A general purpose implementation of the  
955 QM/MM approach and its application to problems in catalysis, *Comp.*  
956 *Theor. Chem.* 632 (2003) 1–28.
- 957 [88] S. Metz, J. Kstner, A. A. Sokol, T. W. Keal, P. Sherwood, Chemshell  
958 – a modular software package for QM/MM simulations, *Wiley Inter-*  
959 *discip. Rev. Comput. Mol. Sci.* 4 (2014) 101–110.
- 960 [89] P. Tosco, L. Lazzarato, Mechanistic insights into cyclooxygenase irre-  
961 versible inactivation by aspirin, *ChemMedChem* 4 (2009) 939–945.
- 962 [90] L. Toth, L. Muszbek, I. Komaromi, Mechanism of the irreversible inhi-  
963 bition of human cyclooxygenase-1 by aspirin as predicted by QM/MM  
964 calculations, *J. Mol. Graphics Modell.* 40 (2013) 99–109.
- 965 [91] S. Ma, L. S. Devi-Kesavan, J. Gao, Molecular dynamics simulations of  
966 the catalytic pathway of a cysteine protease: a combined qm/mm study  
967 of human cathepsin k, *J. Am. Chem. Soc.* 129 (2007) 13633–13645.

- 968 [92] M. Mladenovic, R. F. Fink, W. Thiel, T. Schirmeister, B. Engels, On  
969 the origin of the stabilization of the zwitterionic resting state of cysteine  
970 proteases: a theoretical study, *J. Am. Chem. Soc.* 130 (2008) 8696–  
971 8705.
- 972 [93] K. Arafet, S. Ferrer, S. Martí, V. Moliner, Quantum mechan-  
973 ics/molecular mechanics studies of the mechanism of falcipain-2 inhi-  
974 bition by the epoxysuccinate E64, *Biochemistry* 53 (2014) 3336–3346.
- 975 [94] V. Buback, M. Mladenovic, B. Engels, T. Schirmeister, Rational design  
976 of improved aziridine-based inhibitors of cysteine proteases, *J. Phys.*  
977 *Chem. B* 113 (2009) 5282–5289.
- 978 [95] M. Shokhen, N. Khazanov, A. Albeck, The mechanism of papain in-  
979 hibition by peptidyl aldehydes, *Proteins: Struct., Funct., Bioinf.* 79  
980 (2011) 975–985.
- 981 [96] J. Fanfrlík, P. S. Brahmshatriya, J. Rezac, A. Jílková, M. Horn,  
982 M. Mares, P. Hobza, M. Lepsík, Quantum mechanics-based scoring  
983 rationalizes the irreversible inactivation of parasitic schistosoma man-  
984 soni cysteine peptidase by vinyl sulfone inhibitors, *J. Phys. Chem. B*  
985 117 (2013) 14973–14982.
- 986 [97] A. Latorre, T. Schirmeister, J. Kesselring, S. Jung, P. Johé, U. A.  
987 Hellmich, A. Heilos, B. Engels, R. L. Krauth-Siegel, N. Dirdjaja, et al.,  
988 Dipeptidyl nitroalkenes as potent reversible inhibitors of cysteine pro-  
989 teases rhodesain and cruzain, *ACS Med. Chem. Lett.* 7 (2016) 1073–  
990 1076.
- 991 [98] M. Mladenovic, T. Schirmeister, S. Thiel, W. Thiel, B. Engels, The  
992 importance of the active site histidine for the activity of epoxide-or  
993 aziridine-based inhibitors of cysteine proteases, *ChemMedChem* 2  
994 (2007) 120–128.
- 995 [99] M. Mladenovic, K. Junold, R. F. Fink, W. Thiel, T. Schirmeister,  
996 B. Engels, Atomistic insights into the inhibition of cysteine proteases:  
997 first QM/MM calculations clarifying the regiospecificity and the inhibi-  
998 tion potency of epoxide-and aziridine-based inhibitors, *J. Phys. Chem.*  
999 *B* 112 (2008) 5458–5469.

- 1000 [100] M. Mladenovic, K. Ansorg, R. F. Fink, W. Thiel, T. Schirmeister,  
1001 B. Engels, Atomistic insights into the inhibition of cysteine proteases:  
1002 first QM/MM calculations clarifying the stereoselectivity of epoxide-  
1003 based inhibitors, *J. Phys. Chem. B* 112 (2008) 11798–11808.
- 1004 [101] R. Vicik, H. Helten, T. Schirmeister, B. Engels, Rational design  
1005 of aziridine-containing cysteine protease inhibitors with improved po-  
1006 tency: Studies on inhibition mechanism, *ChemMedChem* 1 (2006)  
1007 1021–1028.
- 1008 [102] R. Vicik, M. Busemann, C. Gelhaus, N. Stiefl, J. Scheiber, W. Schmitz,  
1009 F. Schulz, M. Mladenovic, B. Engels, M. Leippe, K. Baumann,  
1010 T. Schirmeister, Aziridide-based inhibitors of cathepsinL: Synthesis, in-  
1011 hibition activity, and docking studies, *ChemMedChem* 1 (2006) 1126–  
1012 1141.
- 1013 [103] T. Schirmeister, J. Kesselring, S. Jung, T. H. Schneider, A. Weick-  
1014 ert, J. Becker, W. Lee, D. Bamberger, P. R. Wich, U. Distler, et al.,  
1015 Quantum chemical-based protocol for the rational design of covalent  
1016 inhibitors, *J. Am. Chem. Soc.* 138 (2016) 8332–8335.